Biosensors and Bioelectronics 182 (2021) 113188

Contents lists available at ScienceDirect

Biosensors and Bioelectronics

journal homepage: http://www.elsevier.com/locate/bios

AIEgens enabled ultrasensitive point-of-care test for multiple targets of food safety: Aflatoxin B_1 and cyclopiazonic acid as an example

Xiaofeng Hu [a,1], Pengfei Zhang [b,1], Du Wang [a], Jun Jiang [a], Xiaomei Chen [a], Yong Liu [b], Zhaowei Zhang [a,*], Ben Zhong Tang [b,***], Peiwu Li [a,**]

[a] National Reference Laboratory for Agricultural Testing (Biotoxin), Key Laboratory of Biology and Genetic Improvement of Oil Crops, Key Laboratory of Detection for Mycotoxins, Ministry of Agriculture and Rural Affairs, Oil Crops Research Institute of Chinese Academy of Agricultural Sciences, Wuhan 430062, PR China
[b] Department of Chemistry, Hong Kong Branch of Chinese National Engineering Research Center for Tissue Restoration and Reconstruction, The Hong Kong University of Science & Technology, Clear Water Bay, Kowloon, Hong Kong, China

ARTICLE INFO

Keywords:
Aggregation-induced emission
Lateral flow
Point-of-care test
Aflatoxin B_1
Cyclopiazonic acid
Food safety

ABSTRACT

Food safety is currently a significant issue for human life and health. Various fluorescent nanomaterials have been applied in the point-of-care test (POCT) for food safety as labeling materials. However, previous fluorescent nanomaterials can cause aggregation-caused quenching (ACQ), thus reducing the detection sensitivity. Conversely, aggregation-induced emission luminogens (AIEgens) are promising candidates for POCT in the food safety field because they can enhance detection sensitivity and throughput. Mycotoxins, such as aflatoxin B_1 (AFB_1) and cyclopiazonic acid (CPA), are a primary threat to human life and health and a significant food safety issue, and their on-site detection from farm to table is needed. Herein, an ultrasensitive point-of-care test was developed based on TPE-Br, a blue-emissive tetraphenylethylene derivative AIEgen. Under optimal conditions, this AIEgen-based lateral-flow biosensor (ALFB) allowed for a rapid response of 8 min toward AFB_1 and CPA detection, with considerable sensitivities of 0.003 and 0.01 ng/mL in peanut matrices, respectively. In peanut matrices, the recoveries were 90.3%–110.0% for both mycotoxins, with relative standard deviations (RSDs) below 6%. The ALFB was further validated via UPLC-MS/MS using spiked peanut samples. AIEgens open an avenue for on-site, ultrasensitive, high-throughput detection methods and can be extensively used in point-of-care tests in food safety.

1. Introduction

Point-of-care tests (POCTs) provide an on-site and laboratory-independent strategy for extensive applications in food safety (Wu et al., 2017a) and clinical tests (Marquez et al., 2019). As the practical pioneering method in POCTs, paper-based lateral flow immunoassays (LFIAs) possess advantages of rapidity, simplicity, and low cost. Typically, gold nanoparticle (AuNP)-based LFIAs used the human chorionic gonadotropin (HCG) test are a successful application of LFIAs (Tian et al., 2013). However, they provide only a qualitative sample-to-answer, insufficient sensitivity, and narrow linear range due to their restricted colorimetric signal. Fluorescent nanomaterials, such as quantum dots (QDs) (Huang et al., 2016), lanthanide-based microspheres (Xia et al., 2009; Li et al., 2019), upconversion phosphors (You et al., 2017), and photonic crystals (Inan et al., 2017), have been introduced to improve detection sensitivity and work linear range (Li et al., 2010). These fluorescent nanomaterials previously conjugated with specific antibodies were captured by the corresponding antigen on a test line, thus causing aggregation of vast fluorescent nanomaterials. The confinement of superfluous fluorescent nanomaterials on a defined surface of the test line inevitably results in fluorescence quenching due to π–π stacking, other nonradiative pathways, or both, generally recognized as aggregation-caused quenching (ACQ) (Yuan et al., 2010). The ACQ phenomenon hampers the broad application of LFIA-enabled POCTs to practical applications in food safety. The AIE discovery opens a promising avenue for the fluorescence-based detection strategy

* Corresponding authors. Address: No. 2, Xudong 2nd Road, Oil Crops Research Institute of the Chinese Academy of Agricultural Sciences, Wuhan, 430062, China.
** Corresponding authors. Address: No. 2, Xudong 2nd Road, Oil Crops Research Institute of the Chinese Academy of Agricultural Sciences, Wuhan, 430062, China.
*** Corresponding author. Hong Kong Univ Sci & Technol, Chinese Natl Engn Res Ctr Tissue Restorat & Recon, Hong Kong Branch, Dept Chem, Hong Kong, China.
E-mail addresses: zwzhang@whu.edu.cn (Z. Zhang), tangbenz@ust.hk (B.Z. Tang), peiwuli@oilcrops.cn (P. Li).
[1] These authors contributed equally.

https://doi.org/10.1016/j.bios.2021.113188
Received 14 January 2021; Received in revised form 9 March 2021; Accepted 18 March 2021
Available online 20 March 2021

(Hong et al., 2011). AIE phenomena result in weak fluorescence in the solution state but dramatically enhanced emission in the aggregated form due to intramolecular rotation restriction. Due to their substantial luminescence in the aggregated state, AIEgens have been successfully exploited in optoelectronic and biological applications (Hong et al., 2009). Several studies focused on AIEgens have enabled rapid assays to monitor environmental risk (hydrazine) (Song et al., 2017) and terrorists (phosgene) (Xie et al., 2017). However, these demonstrations focused on a single target of interest and used a standard solution other than the real sample. Before AIEgens are used for practical applications in food safety, several challenges should be addressed: (1) multiple targets of interest should be studied due to common co-contamination by chemical residues or metabolites, (2) quantitative detection with a portable reader should be achieved for on-site detection to reduce detection error by the naked eye, and (3) complicated matrix effects should be eliminated. It has much research must still be conducted to use AIEgens in in-field applications.

Aspergillus flavus is an inevitable saprophytic fungus that severely infects grain and oil products worldwide. Under suitable temperature and humidity, up to 60% of *Aspergillus* can produce harmful secondary metabolites (Keller et al., 2005). Mycotoxins are the most toxic compounds among these metabolites and usually co-contaminate a wide range of foods and feed. Typical mycotoxins produced by *Aspergillus flavus* are aflatoxin B_1 (AFB_1) and cyclopiazonic acid (CPA). AFB_1 is a crucial risk factor for liver cancer and was identified as a carcinogen (group 1) by the International Agency for Research on Cancer (IARC) of the World Health Organization (WHO). AFB_1 has caused hundreds of deaths in India and Kenya in a short period (Kumar et al., 2017). The toxicity of CPA is equivalent to that of AFB_1 (Tokuoka et al., 2008). CPA can easily lead to necrosis of the heart, liver, pancreas, and kidney and often contaminates peanuts along with AFB_1.

In 1960, the grave food safety issue that caused 100,000 turkey deaths in the UK could be attributed to AFB_1 and CPA (Spensley, 1963). Worse, CPA and AFT's co-contamination is easily found throughout the whole food chain, including production, harvest, storage, transportation, and digestion (Lee and Hagler, 1991). Therefore, to monitor the multiple mycotoxins produced by *Aspergillus flavus*, the development of a high-sensitivity and high-throughput point-of-care test is urgent. Although HPLC and HPLC-MS/MS have made outstanding contributions in multiple mycotoxin detection and are the typically used techniques (Zhang et al., 2016), POCTs, such as those using lateral flow biosensors (LFBs), as a typical example, has the advantages of simplicity, speed, and specificity and thus has been widely applied in food safety, clinical testing, and environmental monitoring (Bahadir and Sezginturk, 2016; Li and Macdonald, 2016). Various LFB markers, including colloidal gold, magnetic materials, and fluorescent nanoparticles, have been investigated to enhance the sensitivity of LFBs so far. Comparatively, fluorescent LFBs have an advantage over colloidal gold in detection sensitivity (Xie et al., 2014). However, during the detection of ordinary fluorescence LFIC, fluorescent nanoparticles will gather together to form a predesigned detection zone. This aggregation can inevitably lead to the ACQ phenomenon owing to the high local concentration of fluorescent molecules and then seriously reduce the detection sensitivity. Fortunately, AIEgens can address the challenge of the signal reduction from ACQ and improve the detection sensitivity.

Introduction fluorescent molecules into nanoparticles can enhance the sensitivity by coupling or adsorbing numerous fluorescent molecules into one nanoparticle. The ACQ will occur when lots of fluorescent molecules are trapped in one nanoparticle, thus reducing the detection sensitivity. By contrast, AIEgens are the preferred fluorescent nanomaterials because the severely restricted rotation of AIEgens generates strong fluorescence, thus significantly improving detection sensitivity (Mei et al., 2015). The more AIEgens in one nanoparticle, the higher fluorescent intensity can be observed, providing robust fluorescent emission nanoparticles. In this regard, Li et al. developed an AIEgens-based silica nanoparticle, finding the non-fluorescent silole precursor emitted a strong green fluorescence resulting from the AIE phenomena (Li et al., 2013). Furthermore, AIEgens have been assembled into polymer micelle nanoparticles, inducing the highly intensive fluorescence due to limited AIEgens rotation inside the polymer micelle (Wang et al., 2020). These AIEgen-based nanoparticles have been widely used in optoelectronics (Sun et al., 2018), biosensing (Zhang et al., 2018), and biomedical applications (Zhao et al., 2018).

Inspired by the concept of AIEgens, this study used TPE-Br, a typical AIE-active material, to develop AIEgen nanospheres with the swelling method. After conjugation with the antibody, an AIE-based lateral flow biosensor (ALFB) was developed to detect AFB_1 and CPA simultaneously. A homemade novel portable reader was used to quantify the mycotoxin concentration based on the fluorescent signal. After optimization, the powerful performances were evaluated and included the limit of detection (LOD), linear range, recovery, specificity, and intra- and interassay variability. To validate the ALFB, 100 peanut samples that AFB_1 and CPA naturally contaminated were used to compare the AFL biosensor to HPLC-MS/MS. To the best of our knowledge, this is the first study on the quantitative detection of multiple targets in real samples with complex matrix effects based on AIEgen nanospheres and a homemade portable fluorescence reader. Addressing the challenge of ACQ in POCTs, this ALFB shows the merits of ultrasensitivity and high throughput and highlights an avenue for multiple-target monitoring by applying POCTs in food safety.

2. Materials and methods

2.1. Chemicals and instruments

Standard AFB_1, CPA, deoxynivalenol (DON), zearalenone (ZEN), T-2 toxin, fumonisin B_1 (FB_1), ochratoxin A (OTA), diacetoxyscirpenol (DAS), patulin (PAT), and citrinin (CIT) solutions, sodium dodecyl sulfate (SDS), methylene chloride (CH_2Cl_2), *N*-(3-dimethylaminopropyl)-*N*′-ethylcarbodiimide hydrochloride (EDC), boric acid, borax, bovine serum albumin (BSA), AFB_1-BSA, potassium dihydrogen phosphate, disodium phosphate, sodium chloride (NaCl), polyvinylpyrrolidone K30 (PVP K30), sucrose, Tween-20, acetonitrile (ACN) and methanol (MeOH) were purchased from Sigma-Aldrich Co., Ltd. (St. Louis, MO, USA). CPA-ovalbumin (OVA) was produced as our previous work (Yan et al., 2020). Goat anti-mouse immunoglobulin (IgG) was purchased from Wuhan Boster Biological Technology Co., Ltd. (Wuhan, Hubei, China). Carboxyl-modified monodisperse polystyrene nanospheres were purchased from Shanghai Uni Biotechnology Co., Ltd. (Shanghai, China). The absorbent pad, nitrocellulose (NC) membrane (HFC13502), sample pad (fusion five, fusion three, glass fibers GFCP000800), and plastic adhesive card were purchased from Millipore (Billerica, MA, USA), the NC membrane (CN 95) was purchased from Sartorius (Germany), and the NC membrane (FF120HP) was purchased from Whatman International Ltd. (Maidstone, Kent, UK). Ultrapure water was obtained from a Millipore Milli-Q system.

An XYZ 3050 dispensing platform, CM 4000 guillotine cutter, and LM 4000 batch laminator (BioDot, Irvine, CA, USA) were used to prepare the detection strip. A high-speed freezing centrifuge (CF16RX) was obtained from Hitachi (Tokyo, Japan). The vortex oscillator was purchased from VELP Corporation (Bohemia, NY, USA). The LCMS-8060 UPLC-MS/MS system (Shimadzu, Kyoto, Japan) was used to compare the proposed ALFB method.

2.2. Development of the ALF portable reader

We designed a delicate ALFB portable reader driven by a commercially available power supply or rechargeable batteries. The ALFB can be accurately transmitted from the ALF slot to the dark cassette using an electromotor in its drive part. In its optical path design, the AIEgen fluorescence response can be realized in a dark cassette. Exited light is generated by an LED source (365 nm). After the exciting light reaches

the dark cassette, the ALFB is moved evenly, and the light is vertically irradiated on the test line (T line) and control line (C line) of the ALFB. The emitted light is recorded by a photomultiplier tube (PMT) after filtration at 480 nm. All the signals are transmitted to the control system with a touch panel.

2.3. Development of anti-AFB_1 or anti-CPA monoclonal antibody (mAb)

Briefly, antigens of AFB_1 and CPA were coupled to BSA and inoculated by subcutaneous injection into BALB/c mice (7–8 weeks old) at multiple sites. The indirect noncompetitive enzyme-linked immunosorbent assay (inc-ELISA) and indirect competitive ELISA (ic-ELISA) were used to determine the titer and antiserum sensitivity. Cell fusion and hybridoma screening were performed, and then the positive cells were screened in a two-step procedure to guarantee monoclonality. After that, cell fusion and hybridoma screening were performed, and the positive cells were screened in a two-step procedure to ensure monoclonality. Then, the stable clones were expanded to obtain abundant hybridoma cells. After intraperitoneal injection of 0.3 mL of Freund's incomplete adjuvant, each BALB/c mouse was intraperitoneally injected with these hybridoma cells. After the mice showed significant abdominal distention, the ascitic fluids were extracted and purified by caprylic acid-ammonium sulfate precipitation using a protein G immunoaffinity column (IAC) and then stored at −20 °C before use.

2.4. Synthesis of the AIEgen nanospheres

As a typical AIEgen, TPE-Br was synthesized and purified according to previous work with little modification (Feng et al., 2020). The assembly of polystyrene-based TPE-Br nanospheres was performed as follows. A total of 100 mg polystyrene was dispersed in 10 mL of water (containing 0.25% SDS) via ultrasound before 0.5 mL of TPE-Br (mass fraction, 10%) in CH_2Cl_2 was added. After the dispersion was mixed entirely via ultrasound for 1 min, the solution was stirred at 40 °C. CH_2Cl_2 was removed by rotary evaporation, and then AIEgen (TPE-Br) nanospheres were collected by centrifugation. The resulting AIEgen nanospheres were washed three times with water to remove SDS. They were further washed and centrifuged several times with ethanol until no fluorescence was observed in the supernatant. Finally, fluorescent AIEgen nanospheres were dried and redispersed in the water at a 2 mg/mL concentration before further use.

2.5. Preparation of mAb@AIEgen nanospheres

EDC and NHS were used to prepare active nanospheres with carboxyl groups in aqueous media. First, 200 μL of AIEgen nanospheres was dispersed in 800 μL of PBS buffer (0.01 mol/L, pH 7.4) via ultrasound for 2 min. Then, 20 μL of EDC (10, 20, 40, 50, and 60 mg/mL) and 20 μL of NHS (10, 20, 40, 50, and 60 mg/mL) were added and stirred for 15 min, followed by centrifugation at 17,000 g for 20 min. The precipitate was resuspended in 1.0 mL of boric acid buffer (pH 6.5, 7.0, 7.4, 7.8, 8.2, 8.7, 9.0, and 9.5). After that, 1 mg/mL mAb (AFB_1 or CPA) was dispersed in PBS buffer (0.01 mol/L, pH 7.4). A gradient of mAbs (AFB_1 or CPA) (5, 10, 20, 30, 40, and 50 μL) was added, and the solution was vortexed (30, 60, 90, 120, 150, 180, and 240 min) before centrifugation at 17,000 g for 20 min. The residue was resuspended in 1.0 mL of PBS buffer (pH 7.4, containing 0.5% BSA). The prepared mAb@AIEgen nanospheres (AFB_1 or CPA) were stored at 4 °C for future use.

2.6. Assembly of the ALFB

Owing to its good biocompatibility and excellent protein adsorption performance, the NC membrane has been widely used in paper-based flow chromatography test strips (Ratajczak and Stobiecka, 2020). The ALFB consists of an NC membrane, a plastic backing plate, a sample pad, and an absorbent pad. First, a BioDot XYZ 3050 dispensing platform operated at dispensing rates of 0.3, 0.5, and 0.7 μL/cm was used to spray AFB_1-BSA (0.1, 0.2, 0.25, 0.5, and 0.7 mg/mL), CPA-OVA (0.1, 0.2, 0.25, 0.5, and 0.7 mg/mL), and goat anti-mouse IgG (0.1, 0.2, 0.3, and 0.4 mg/mL) on NC membranes for use as the T1 line (AFB_1), T2 line (CPA) and C line (IgG), respectively. Six and four mm were set as the distances between the C and T1 lines and the T1 and T2 lines. After drying at 37 °C for 30 min, the absorbent pad, NC membrane (Whatman 120, Millipore 135, Sartorius N95), and sample pad (fusion 3, fusion 5, and glass fibers) were sequentially attached to the plastic backing plate. Every part was overlapped with 2 mm to ensure solution migration along the strip. Finally, the whole assembly of the scale board was cut into strips with a 4.0 mm width using a guillotine cutter and preserved at 4 °C.

2.7. Sample treatment for the ALFB or UPLC-MS/MS

Peanut samples were used for experimental validation. Modified one-step sample treatment was performed according to previous work (Hu et al., 2016). First, 10 g of peanut sample was added to 20 mL of methanol/water (70:30, v/v) containing 4% NaCl and homogenized for 2 min. Then, the mixture was filtered with glass fiber filter paper. For the ALFB, the filtrate was diluted three times with a running buffer before the test. For UPLC-MS/MS, the filtrate was further filtered with a 0.22 μm organic phase filter before a determination by UPLC-MS/MS.

2.8. Validation of the ALFB

The calibration curve, LOD, linear range, specificity, stability, inter- or intraassay variability, and recovery were evaluated via a spiked peanut sample. For the standard curve, the correlation was established as $Y = aX + b$. Y represents the ratio of the fluorescence intensity of the T line and C line, and X represents the common logarithm of the AFB_1 or CPA concentration. For the LOD, 40 blank peanut samples were tested, and the LODs were calculated via the formula "$LOD = 3\delta/s$" (Wu et al., 2017b), in which "δ" is the standard deviation of the 40 blank sample values, while "s" represents the sensitivity of the method, that is, the slope of the calibration curve (Long and Winefordner, 1983). For specificity, AFB_1, CPA, and eight other mycotoxins (DON, ZEN, T-2, FB_1, OTA, DAS, PAT, and CIT) with a concentration of 100 ng/mL were examined on the strip individually. Peanut samples spiked with AFB_1 (2.0 μg/kg) and CPA (30.0 μg/kg) were introduced to evaluate the interassay and intraassay variability. The coefficient of variation (CV) of the readout values from six ALFBs of different batches and six ALFBs from the same batch was used to assess the interassay and intraassay variability. The same spiked sample was used to evaluate the ALFB stability by testing the ALFBs every five days upon storage at 4 °C and room temperature. Spiked peanut samples (AFB_1: 0.1, 5, and 20 μg/kg; CPA: 20, 100, and 700 μg/kg) were employed for the recovery test.

2.9. Application

For its applications in the real samples, 100 peanut samples were analyzed via ALFB and UPLC-MS/MS methods. Peanut samples from No. 1–40 were commercially available vacuum-packed peanuts from local markets, while the ones from No. 41–100 were previously collected from markets and farmers between 2016 and 2020. The results of the ALFB and UPLC-MS/MS (LCMS-8060, Shimadzu: multiple reaction monitoring modes) methods were compared. Chromatographic separation was performed using a Thermo C18 column (2.7 μm, 10 cm) without a guard column at 40 °C. Mobile phase A is water, and mobile phase B is methanol. A linear gradient elution program was developed and used mobile phases A and B with the following conditions: 0–2 min, 30–70% B; 2–3 min, 70% B; 3–4 min, 70–30% B; 4–5 min, 30% B. The elution flow rate was set at 300 μL/min, the injection volume was 1 μL, and the run time was 5 min. Spectra were obtained using a triple quadrupole coupled with an electrospray interface (ESI). The MS/MS system was operated using ESI sources in positive or negative mode. Ion pair

parameters are shown in Table S1. The conditions were set as follows: capillary voltage, 3.0 kV for ESI^+ and −3.0 kV for ESI^-; extractor voltage, 3.0 V; source temperature, 150 °C; desolvation temperature, 350 °C. Argon was used as the collision gas (collision cell, 0.8 V), and nitrogen was used as both the nebulizing (50 L/h) and desolvation gases (650 L/h). Data were acquired using LabSolution software (Version 5.89).

3. Results and discussion

3.1. Characterization of TPE-Br-nanospheres

AIEgens were faintly emissive when dispersed in solution but showed strong fluorescence in the aggregate state (Fig. 1a). The polystyrene nanospheres were swollen for loading TPE-Br by ultrasound in CH_2Cl_2. After CH_2Cl_2 was removed by rotary evaporation, TPE-Br was sealed inside the polystyrene nanospheres when the polystyrene nanospheres' pore size returned to their original diameter (Fig. 1b). The morphology of the TPE-Br nanospheres was observed by using transmission electron microscopy (TEM). The TPE-Br nanospheres were mostly spherical in morphology, with good dispersion and an average diameter of approximately 60 nm (Fig. 1f). The optical properties of the TPE-Br nanospheres were confirmed by UV–Vis and fluorescence spectroscopy. The typical excitation and emission wavelengths of the TPE-Br nanospheres were 365 nm and 480 nm, respectively (Fig. 1g). The massive Stokes shift of 200 nm can efficiently avoid interference between the excitation and emission signals. The insert in Fig. 1g shows the color of the TPE-Br-nanosphere solution under visible light (white) and UV light (blue). These results confirmed that the successful preparation method of TPE-Br nanospheres could be used to fabricate biosensors.

3.2. Optimization of the conjugation of TPE-Br-Nanospheres to antibodies

Optimization of the pH value for TPE-Br nanospheres and antibody conjugation. Different pH values of boric acid buffer solutions were used to optimize the pH value for conjugating TPE-Br nanospheres with Ab. The ratio of the fluorescence intensity of the T-line and C-line (F_T/F_C) increased with increasing the pH to 6.5 and then decreased with increasing the pH above 8.2 (Fig. S1). Thus, the optimal pH value was 8.2.

Optimization of the mAb dose. The loading amount of anti-AFB_1 mAb or anti-CPA mAb on the NC membrane plays a vital role in

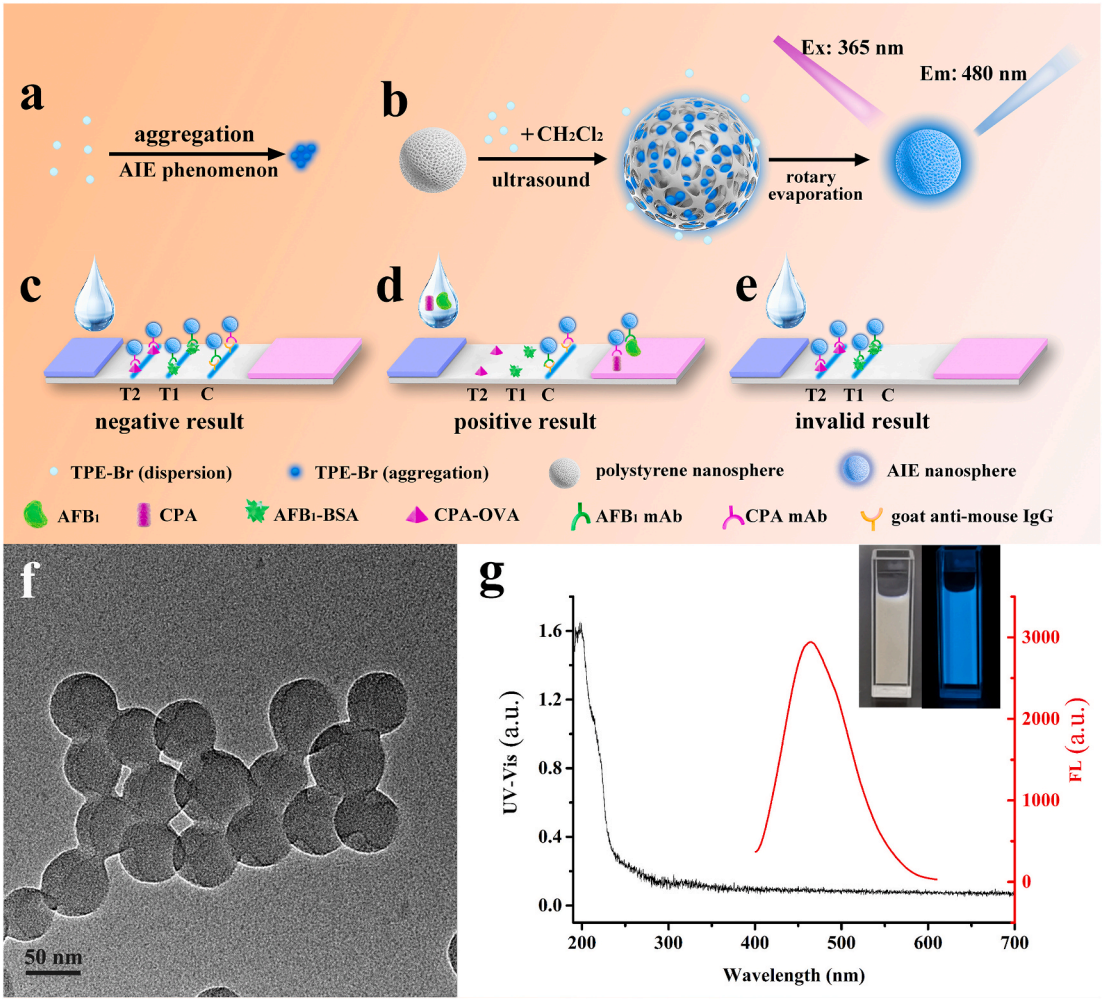

Fig. 1. (a) The AIEgen principle (Left: no fluorescence without TPE-Br aggregation; high fluorescence with TPE-Br aggregation). (b) Synthesis of TPE-Br nanosphere. From left to right: polystyrene nanosphere before TPE-Br swelling, swelled polystyrene nanosphere to trap TPE-Br, and polystyrene nanosphere swelled by TPE-Br, showing strong AIE fluorescences. The principle of AIEgen-based lateral flow biosensor (ALFB) for aflatoxin B_1 (AFB_1) and cyclopiazonic acid (CPA): (c) negative result without AFB_1 or CPA; (d) positive result with both AFB_1 and CPA; (e) invalidated result (no show of control line). (f) Transmission electron microscopy (TEM) image of AIEgen (TPE-Br) nanospheres. (g) UV–Vis absorption (black), fluorescence emission (red) spectra of AIEgen (TPE-Br) nanospheres; insert: digital photos of under visible light (left) and UV light (right). (For interpretation of the references to color in this figure legend, the reader is referred to the Web version of this article.)

improving the sensitivity and linear range. Increasing the dose of anti-AFB_1 mAb or anti-CPA mAb can increase the test line's fluorescence intensity during the detection of negative samples and allow a more comprehensive linear dynamic range. Decreasing the dose of the two mAbs can induce a lower limit of detection but cause a lower fluorescence intensity. The results suggested that 10 ng and 20 ng of anti-AFB_1 mAb and anti-CPA mAb, respectively, were the optimized doses to ensure clear test lines and reduce background interference.

3.3. Optimization of the ALFB

The following parameters were optimized to obtain better sensitivity and stability: (a) the dosage of the antigen and IgG on the test zone; (b) the NC membrane; (c) the spray rate; and (d) the sample pad. According to the AIEgen fluorescence intensity and sharpness of the test line and control line, the following experimental conditions were applied as the optimized conditions: (a) AFB_1-BSA, CPA-OVA, and goat anti-mouse IgG concentrations of 0.25, 0.5, and 0.2 mg/mL, respectively; (b) a Millipore HFC13502 NC membrane; (c) a spray rate of 0.5 μL/cm; and (d) a sample

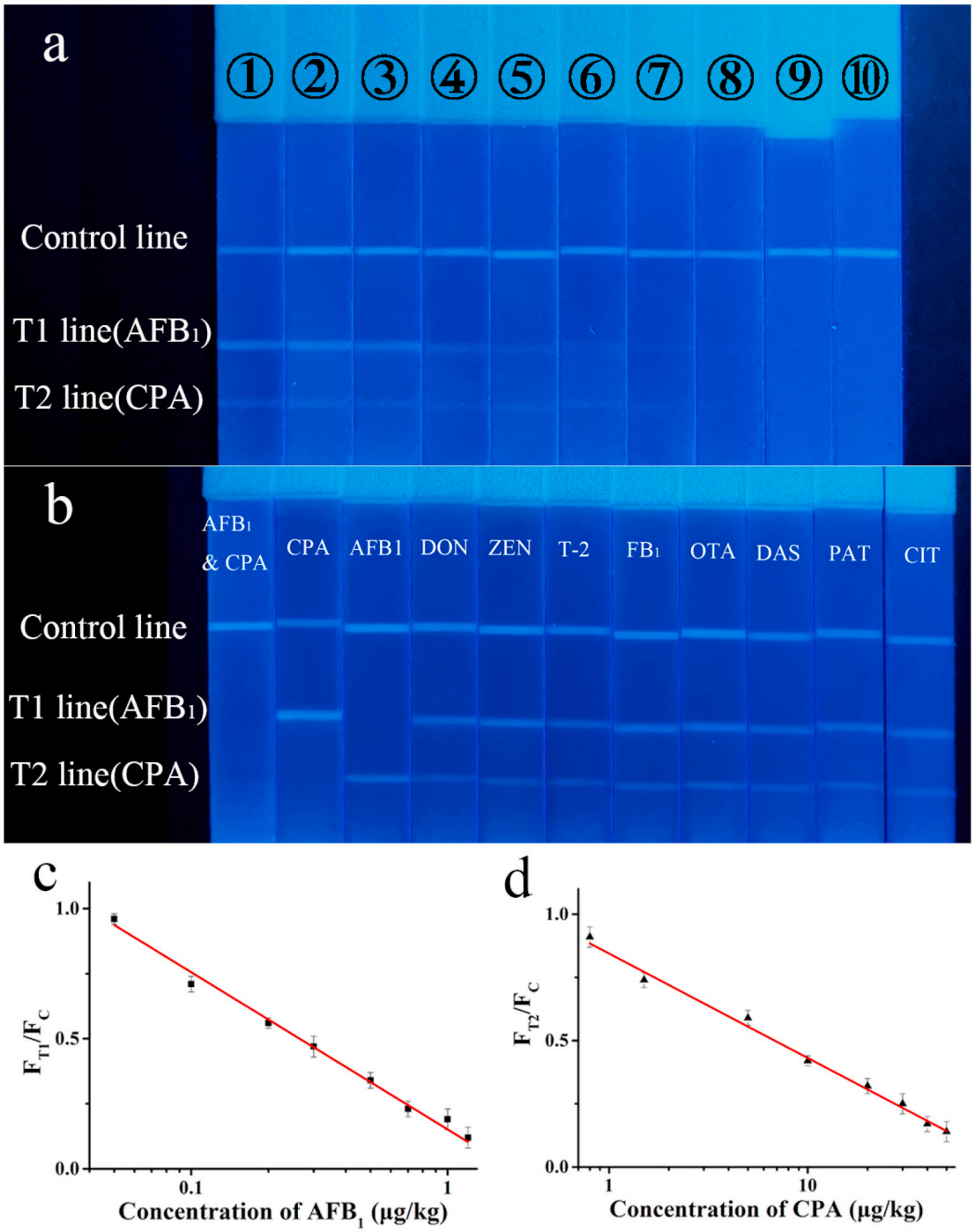

Fig. 2. (a) Photo images for the AIEgen-based lateral flow biosensor (ALFB) with the increasing concentration of AFB_1 (from ① to ⑩: 0, 0.05, 0.1, 0.2, 0.3, 0.4, 0.5, 1.0, 2.0, and 3.0 ng/mL) and CPA(from ① to ⑩: 0, 0.8, 1.5, 5, 10, 15, 20, 30, 40, and 50 ng/mL) in peanut sample; (b) specificity results in different interfering mycotoxins: deoxynivalenol (DON), zearalenone (ZEN), T-2 toxin, fumonisin B_1 (FB_1), ochratoxin A (OTA), diacetoxyscirpenol (DAS), patulin (PAT) and citrinin (CIT); Calibration curve of (c) aflatoxin B_1 (AFB_1) and (d) cyclopiazonic acid (CPA), each data represented the average value from three measurements.

pad (fusion five).

3.4. ALFB test procedure

As a competitive reaction, the mAb@AIEgen nanospheres (1 μL) and sample extract were premixed in a microwell at room temperature for 1 min. Then, the ALFB was inserted into the microwell and incubated at 37 °C. The running buffer was optimized as a mixture of 1% BSA+ 1% Tween-20 + 1% sucrose in PBS buffer (0.01 M, pH 7.4). The incubation time was optimized as 6 min. For AFB_1- and/or CPA-positive samples, mAb@AIEgen nanospheres reacted with AFB_1 and/or CPA in the microwell to form an immunocomplex. Then, the excess mAb@AIEgen nanospheres were captured by the test line. On the control line, the preloaded rabbit anti-mouse IgG captured the remaining mAb@AIEgen nanospheres. After that, the fluorescence intensities of the T and C lines were recorded under the excitation of 365 nm. When the fluorescence intensity of the C line was stable, the higher concentration of AFB_1/CPA resulted in the lower fluorescent intensity on T1/T2 lines (Fig. 2a).

The result can be obtained by the naked eye or a portable reader (Fig. 3). For qualitative detection, the naked eye was used via UV light at 365 nm. Only the C line changed to blue for the positive sample (Fig. 1d), but the negative sample resulted in two or three blue lines (Fig. 1c) except for the invalid result without blue C lines (Fig. 1e). For quantitative detection, the fluorescence intensity of the T and C lines should be tested by a portable fluorescence strip reader. The standard curve was established by plotting F_T/F_C against the common logarithm of mycotoxins concentration. Based on inhibition rates and corresponding standard concentrations, a linear equation was used to calculate the concentrations of AFB_1 or CPA.

3.5. ALFB validation

For the LOD, the mean value of 5 repeated experiments was recorded in 20 blank peanut samples. Based on the sample standard curve, the AFB_1 concentration was further calculated and defined as the LOD. The LODs were 0.003 ng/mL and 0.01 ng/mL for the peanut matrices, and the linear range was 0.05–1.2 ng/mL (Fig. 2c, $y = -0.5849x+0.1624$, $R^2 = 0.9928$) and 0.8–50.0 ng/mL (Fig. 2d, $y = -0.4162x+0.8513$, $R^2 = 0.9938$) for AFB_1 and CPA, respectively. Compared with similar reported rapid assays, these AFB_1 and CPA LODs were up to 196 and 600 times larger than those of the reported method (Table 1), respectively (Guo et al., 2019; Hossain et al., 2019; Liu et al., 2020; Song et al., 2014). The sensitivity fulfilled the real application in mycotoxin monitoring by authorities in major countries.

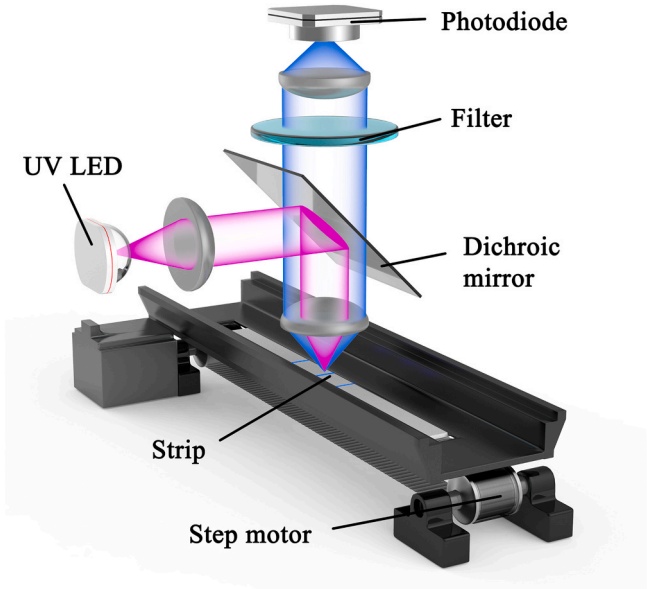

Fig. 3. Design of the optical path and step motor in the portable reader.

Table 1
The comparison of the ALFB with other rapid assays.

No.	Method	LOD		Matrix	Ref.
		AFB1	CPA		
1	Lateral flow immunoassays	0.59 μg/kg	–	Cereal	Liu et al. (2020)
2	Surface plasmon resonance assay	–	6 μg/kg	Cheese	Hossain et al. (2019)
3	Immunochromatographic assay	51 pg/mL	–	Dark soy sauce	Guo et al. (2019)
4	Lateral Flow Immunoassay	0.05 μg/kg	–	Cereal	Song et al. (2014)
5	ALFB	0.003 μg/kg	0.01 μg/kg	Peanut	This work

The specificities of the proposed ALFB for AFB_1 and CPA were tested by comparing their visual and fluorescence signals with those of other common mycotoxins in agro-food. DON, ZEN, T-2, FB_1, OTA, DAS, PAT, and CIT were selected as nonspecific mycotoxins. Each mycotoxin at 100 ng/mL was prepared for the ALFB. All eight interfering mycotoxins were secondary metabolites produced by various fungi, and all of them had specific toxicity. The visual detection results (Fig. 2b) display only the control line for the AFB_1 and CPA groups and two light bands for the other eight mycotoxins. The corresponding fluorescence spectra showed that the positive groups (AFB_1 or CPA) were much lower than the negative mycotoxin groups. These results reveal that the ALFB has good selectivity toward AFB_1 and CPA detection.

For reproducibility, six batches of ALFBs were employed in an interassay recovery procedure (Table S2). The recoveries of AFB_1 and CPA were 95.5%–111.5% and 95.2%–109.9%, respectively. The CVs of 6.7% and 5.1% for AFB_1 and CPA, respectively, indicated their excellent reproducibility. The intraassay experiment was conducted similarly to the interassay. A spiked peanut sample was detected six times by using a same-batch ALFB (Table S3). The recoveries of AFB_1 and CPA were found to be 95.5%–106.5% and 89.5%–98.5%, respectively, with CVs of 4.6% and 4.2%, respectively. The above result indicated that the ALFB method had good repeatability.

To evaluate its stability, the ALFB was stored at 4 °C and tested every 30 days. The fluorescent intensity on T and C lines changed slightly (Fig. 4a), indicating that the ALFB is stable for 180 days when stored at 4 °C. For its actual application, we further tested the ALFB at room temperature. The ALFB showed a negligible change in the test line intensity ratio and control line after storage for 30 days at room temperature (Fig. 4b). These results indicated the considerable stability of the ALFB. Thus, the ALFB storage periods were 30 at room temperature or 180 days at 4 °C, and the ALFB can be distributed and operated in low-resource settings without a cold chain.

Under optimal conditions, the ALFB recoveries were measured by spiking peanut samples with AFB_1 concentrations of 0.05, 5, and 20 μg/kg and CPA concentrations of 20, 100, and 700 μg/kg. The recoveries ranged from 90.3% to 110.0%, with the RSDs below 6% (Table 2). The recovery results fulfilled the requirements for the simultaneous determination of multiple mycotoxins.

3.6. Application

We used ALFB to detect multiple mycotoxins in 100 peanut samples for practical application, while the results via ALFB and UPLC-MS/MS were compared for ALFB validation. Among the 100 peanut samples, 40 peanut samples were purchased from local markets, and 60 peanut samples were collected between 2016 and 2020. Besides, the UPLC-MS/MS method, used as the authority detection method, was also used to

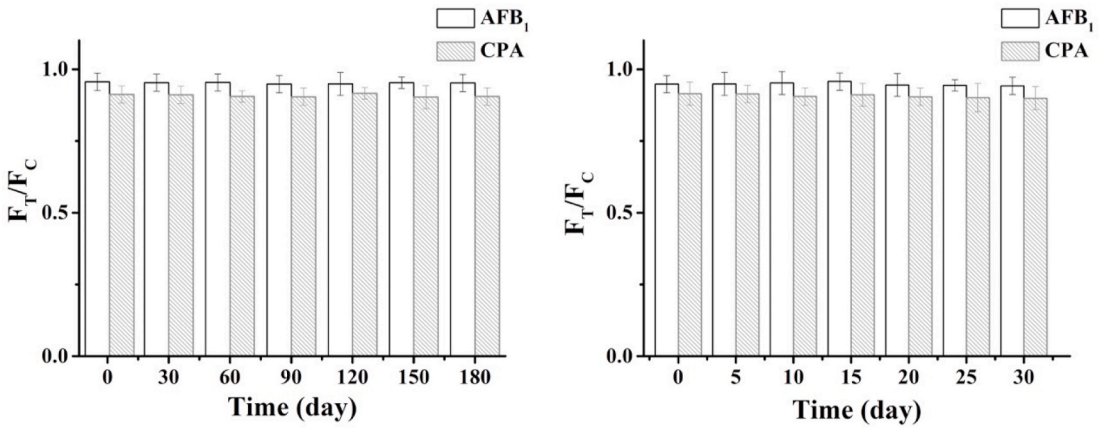

Fig. 4. The stability results of AIEgen-based lateral flow biosensor (ALFB) at (a) 4 °C and (b) room temperature. The F_T/F_C values were recorded from 0.948 to 0.956 at 4 °C for 180 days and from 0.942 to 0.957 at room temperature for 30 days. Results suggested ALFB satisfying stability.

Table 2
Recoveries of the AFLB in peanut samples.

mycotoxin	Spike μg/Kg	Recovery 1 %	Recovery 2 %	Recovery 3 %	RSD %
AFB_1	0.05	102.0	104.0	110.0	4.0
	5	101.0	95.3	107.0	5.8
	20	98.2	93.4	99.3	3.2
CPA	20	98.3	89.3	94.7	4.8
	100	97.2	90.3	89.5	4.6
	700	90.4	97.5	92.5	3.9

detect these peanuts and compared to the proposed ALFB method. Comparing the detection results indicated excellent agreement between these two methods, suggesting that the ALFB can be an alternative to UPLC-MS/MS. (Table 3). Interestingly, both AFB_1 and CPA were found in the peanut samples. Approximately 14% (14/100) of the peanut samples were contaminated by AFB_1 or CPA, while only 5% (5/100) of those samples were contaminated with AFB_1 and CPA.

Table 3
Determination for AFB_1 and CPA in peanut samples via AFLB and UPLC-MS/MS for peanuts.

Sample No.	AFLB method (μg/Kg)		UPLC-MS method (μg/Kg)	
	AFB_1	CPA	AFB_1	CPA
1	3.4	17.0	3.6	17.4
2	6.6	ND[a]	7.1	ND
3	22.2	ND	22.1	ND
41	7.6	ND	7.7	ND
52	6.9	5.2	7.0	5.7
59	ND	3.8	ND	3.5
70	10.1	ND	10.1	ND
74	9.1	7.4	9.2	7.9
75	14.3	ND	15.4	ND
76	ND	7.3	ND	7.7
81	4.4	5.8	4.5	6.4
88	6.3	ND	5.9	ND
93	5.3	ND	5.1	ND
95	16.5	15.5	17.0	15.9
Other samples	N.D.	N.D.	N.D.	N.D.

[a] ND: not detected.

4. Conclusions

Multiple target detection is an effective solution in food safety. Here, AIEgens were introduced to enhance detection sensitivity and throughput, with a sample-to-answer time of 6 min achieved by the naked eye or a portable reader. In detecting multiple mycotoxins in food, the ALFB combined the benefits of sensitive AIEgens and lateral flow to avoid ACQ. First, by assembling TPE with polystyrene nanospheres, very bright AIEgen nanospheres were synthesized. Then, the mAb@AIEgen nanospheres were used in the lateral flow biosensor via a competitive immunoassay. Third, a homemade portable reader was developed for the simultaneous detection of AFB_1 and CPA. The LODs were 0.003 ng/mL and 0.01 ng/mL, with linear ranges of 0.05–1.2 ng/mL and 0.8–50.0 ng/mL for AFB_1 and CPA, respectively. The ALFB also exhibited satisfactory recovery (90.3%~110.0%), selectivity, repeatability, and reproducibility. The results suggested that the ALFB was stable after 30 days at room temperature and 180 days at 4 °C, indicating that the ALFB is a promising candidate for real applications in food safety. Satisfactory compliance was recorded by comparing the ALFB and UPLC-MS/MS. With the various merits of the ALFB, this method holds great promise for applications in food safety.

CRediT authorship contribution statement

Xiaofeng Hu: Methodology, Investigation, Data curation, Writing – Original, Visualization. **Pengfei Zhang:** Investigation, Data curation, Writing - Original. **Du Wang:** Software Programming, Data curation. **Jun Jiang:** Formal analysis, Visualization. **Xiaomei Chen:** Validation, Resources. **Yong Liu:** Resources. **Zhaowei Zhang:** Conceptualization Ideas, Methodology, Writing – review & editing, Supervision, Project, Funding. **Ben Zhong Tang:** Conceptualization Ideas, Supervision. **Peiwu Li:** Project, Funding.

Declaration of competing interest

The authors declare that they have no known competing financial interests or personal relationships that could have appeared to influence the work reported in this paper.

Acknowledgment

Authors thanks for the financial support by the National Key Research and Development Program of China (2018YFC1602500), National Natural Science Foundation of China (32072331), the Research Grants Council of Hong Kong (Nos. 16305618, 16305518, N-HKUST609/19, C6009-17G, and AoE/P-02/12), the Innovation and Technology Commission (No. ITC-CNERC14SC01).

Pengfei Zhang works at Guangdong Key Laboratory of Nanomedicine, Shenzhen Engineering Laboratory of Nanomedicine and Nanoformulations, CAS Key Laboratory of Health Informatics, Institute of Biomedicine and Biotechnology, Shenzhen Institutes of Advanced

Technology, Chinese Academy of Sciences, Shenzhen, 518055, China. Yong Liu works at AIE Institute, Guangzhou Development District, Huangpu, Guangzhou, 510530, China.

Appendix A. Supplementary data

Supplementary data to this article can be found online at https://doi.org/10.1016/j.bios.2021.113188.

References

Bahadir, E.B., Sezginturk, M.K., 2016. Lateral flow assays: principles, designs and labels. Trac-trend Anal. Chem. 82, 286–306.

Feng, A., Jiang, F., Huang, G., Liu, P., 2020. Synthesis of the cationic fluorescent probes for the detection of anionic surfactants by electrostatic self-assembly. Spectrochim. Acta A 224, 117446.

Guo, L., Shao, Y.N., Duan, H., Ma, W., Leng, Y.K., Huang, X.L., Xiong, Y.H., 2019. Magnetic quantum dot nanobead-based fluorescent immunochromatographic assay for the highly sensitive detection of aflatoxin B_1 in dark soy sauce. Anal. Chem. 91 (7), 4727–4734.

Hong, Y., Lam, J.W.Y., Tang, B.Z., 2009. Aggregation-induced emission: phenomenon, mechanism and applications. Chem. Commun. (29), 4332–4353.

Hong, Y., Lam, J.W.Y., Tang, B.Z., 2011. Aggregation-induced emission. Chem. Soc. Rev. 40 (11), 5361–5388.

Hossain, Z., Busman, M., Maragos, C.M., 2019. Immunoassay utilizing imaging surface plasmon resonance for the detection of cyclopiazonic acid (CPA) in maize and cheese. Anal. Bioanal. Chem. 411 (16), 3543–3552.

Hu, X., Hu, R., Zhang, Z., Li, P., Zhang, Q., Wang, M., 2016. Development of a multiple immunoaffinity column for simultaneous determination of multiple mycotoxins in feeds using UPLC-MS/MS. Anal. Bioanal. Chem. 408 (22), 6027–6036.

Huang, X.L., Aguilar, Z.P., Xu, H.Y., Lai, W.H., Xiong, Y.H., 2016. Membrane-based lateral flow immunochromatographic strip with nanoparticles as reporters for detection: a review. Biosens. Bioelectron. 75, 166–180.

Inan, H., Poyraz, M., Inci, F., Lifson, M.A., Baday, M., Cunningham, B.T., Demirci, U., 2017. Photonic crystals: emerging biosensors and their promise for point-of-care applications. Chem. Soc. Rev. 46 (2), 366–388.

Keller, N.P., Turner, G., Bennett, J.W., 2005. Fungal secondary metabolism - from biochemistry to genomics. Nat. Rev. Microbiol. 3 (12), 937–947.

Kumar, P., Mahato, D.K., Kamle, M., Mohanta, T.K., Kang, S.G., 2017. Aflatoxins: a global concern for food safety, human health and their management. Front. Microbiol. 7, 2170.

Lee, Y.J., Hagler, W.M., 1991. Aflatoxin and cyclopiazonic acid production by *Aspergillus flavus* isolated from contaminated maize. J. Food Sci. 56 (3), 871–872.

Li, G., Xu, L., Wu, W., Wang, D., Jiang, J., Chen, X., Zhang, W., Poapolathep, S., Poapolathep, A., Zhang, Z., Zhang, Q., Li, P., 2019. On-Site ultrasensitive detection paper for multiclass chemical contaminants via universal bridge-antibody labeling: mycotoxin and illegal additives in milk as an example. Anal. Chem. 91 (3), 1968–1973.

Li, J., Macdonald, J., 2016. Multiplexed lateral flow biosensors: technological advances for radically improving point-of-care diagnoses. Biosens. Bioelectron. 83, 177–192.

Li, M., Lam, J.W.Y., Mahtab, F., Chen, S., Zhang, W., Hong, Y., Xiong, J., Zheng, Q., Tang, B.Z., 2013. Biotin-decorated fluorescent silica nanoparticles with aggregation-induced emission characteristics: fabrication, cytotoxicity and biological applications. J. Mater. Chem. B 1 (5), 676–684.

Li, Z., Wang, Y., Wang, J., Tang, Z., Pounds, J.G., Lin, Y., 2010. Rapid and sensitive detection of protein biomarker using a portable fluorescence biosensor based on quantum dots and a lateral flow test strip. Anal. Chem. 82 (16), 7008–7014.

Liu, Z.W., Hua, Q.C., Wang, J., Liang, Z.Q., Li, J.H., Wu, J.X., Shen, X., Lei, H.T., Li, X.M., 2020. A smartphone-based dual detection mode device integrated with two lateral flow immunoassays for multiplex mycotoxins in cereals. Biosens. Bioelectron. 158, 112178.

Long, G.L., Winefordner, J.D., 1983. Limit of detection. A closer look at the IUPAC definition. Anal. Chem. 55 (7), 712A–724A.

Marquez, A., Aymerich, J., Dei, M., Rodriguez-Rodriguez, R., Vazquez-Carrera, M., Pizarro-Delgado, J., Gimenez-Gomez, P., Merlos, A., Teres, L., Serra-Graelles, F., Jimenez-Jorquera, C., Dominguez, C., Munoz-Berbel, X., 2019. Reconfigurable multiplexed point of care system for monitoring type 1 diabetes patients. Biosens. Bioelectron. 136, 38–46.

Mei, J., Leung, N.L.C., Kwok, R.T.K., Lam, J.W.Y., Tang, B.Z., 2015. Aggregation-induced emission: together we shine, united we soar! Chem. Rev. 115, 11718–11940.

Ratajczak, K., Stobiecka, M., 2020. High-performance modified cellulose paper-based biosensors for medical diagnostics and early cancer screening: a concise review. Carbohydr. Polym. 229, 115463.

Spensley, P.C., 1963. Aflatoxin, the active principle in Turkey 'X' disease. Endeavour 22, 75–79.

Song, S.Q., Liu, N., Zhao, Z.Y., Ediage, E.N., Wu, S.L., Sun, C.P., De Saeger, S., Wu, A.B., 2014. Multiplex lateral flow immunoassay for mycotoxin determination. Anal. Chem. 86 (10), 4995–5001.

Song, Y., Zong, L., Zhang, L., Li, Z., 2017. To form AIE product with the target analyte: a new strategy for excellent fluorescent probes, and convenient detection of hydrazine in seconds with test strips. Sci. China Chem. 60 (12), 1596–1601.

Sun, N., Su, K., Zhou, Z., Yu, Y., Tian, X., Wang, D., Zhao, X., Zhou, H., Chen, C., 2018. AIE-active polyamide containing diphenylamine-TPE moiety with superior electrofluorochromic performance. ACS Appl. Mater. Interfaces 10 (18), 16105–16112.

Tian, X., Zhu, M., Du, L., Wang, J., Fan, Z., Liu, J., Zhao, Y., Nie, G., 2013. Intrauterine inflammation increases materno-fetal transfer of gold nanoparticles in a size-dependent manner in murine pregnancy. Small 9 (14), 2432–2439.

Tokuoka, M., Seshime, Y., Fujii, I., Kitamoto, K., Takahashi, T., Koyama, Y., 2008. Identification of a novel polyketide synthase-nonribosomal peptide synthetase (PKS-NRPS) gene required for the biosynthesis of cyclopiazonic acid in Aspergillus oryzae. Fungal Genet. Biol. 45 (12), 1608–1615.

Wang, J., Li, J., Wang, L., Han, T., Wang, D., Tang, B.Z., 2020. AIEgen-based polymer nanocomposites for imaging-guided photothermal therapy. ACS Appl. Polym. Mater. 2 (10), 4306–4318.

Wu, M.Y.C., Hsu, M.Y., Chen, S.J., Hwang, D.K., Yen, T.H., Cheng, C.M., 2017a. Point-of-care detection devices for food safety monitoring: proactive disease prevention. Trends Biotechnol. 35 (4), 288–300.

Wu, X., Song, Y., Yan, X., Zhu, C., Ma, Y., Du, D., Lin, Y., 2017b. Carbon quantum dots as fluorescence resonance energy transfer sensors for organophosphate pesticides determination. Biosens. Bioelectron. 94, 292–297.

Xia, X., Xu, Y., Zhao, X., Li, Q., 2009. Lateral flow immunoassay using europium chelate-loaded silica nanoparticles as labels. Clin. Chem. 55 (1), 179–182.

Xie, H., Wu, Y., Zeng, F., Chen, J., Wu, S., 2017. An AIE-based fluorescent test strip for the portable detection of gaseous phosgene. Chem. Commun. 53 (70), 9813–9816.

Xie, Q.Y., Wu, Y.H., Xiong, Q.R., Xu, H.Y., Xiong, Y.H., Liu, K., Jin, Y., Lai, W.H., 2014. Advantages of fluorescent microspheres compared with colloidal gold as a label in immunochromatographic lateral flow assays. Biosens. Bioelectron. 54, 262–265.

Yan, T., Zhang, Z., Zhang, Q., Tang, X., Wang, D., Hu, X., Zhang, W., Chen, X., Li, P., 2020. Simultaneous determination for *A. flavus*–metabolizing mycotoxins by time-resolved fluorescent microbead or gold-enabling test strip in agricultural products based on monoclonal antibodies. Microchim. Acta 187 (12), 653.

You, M., Lin, M., Gong, Y., Wang, S., Li, A., Ji, L., Zhao, H., Ling, K., Wen, T., Huang, Y., Gao, D., Ma, Q., Wang, T., Ma, A., Li, X., Xu, F., 2017. Household fluorescent lateral flow strip platform for sensitive and quantitative prognosis of heart failure using dual-color upconversion nanoparticles. ACS Nano 11 (6), 6261–6270.

Yuan, W.Z., Lu, P., Chen, S., Lam, J.W.Y., Wang, Z., Liu, Y., Kwok, H.S., Ma, Y., Tang, B. Z., 2010. Changing the behavior of chromophores from aggregation-caused quenching to aggregation-induced emission: development of highly efficient light emitters in the solid state. Adv. Mater. 22 (19), 2159–2163.

Zhang, N., Chen, H., Fan, Y., Zhou, L., Trépout, S., Guo, J., Li, M.H., 2018. Fluorescent polymersomes with aggregation-induced emission. ACS Nano 12 (4), 4025–4035.

Zhang, Z., Hu, X., Zhang, Q., Li, P., 2016. Determination for multiple mycotoxins in agricultural products using HPLC-MS/MS via a multiple antibody immunoaffinity column. J. Chromatogr. B 1021, 145–152.

Zhao, J., Dong, Z., Cui, H., Jin, H., Wang, C., 2018. Nanoengineered peptide-graftedhyperbranched polymers for killing of bacteria monitored in real time via intrinsic aggregation-induced emission. ACS Appl. Mater. Interfaces 10 (49), 42058–42067.